ISSN 0976 – 1411

Available online at www.internationaleJournals.com

International eJournals

International eJournal of Mathematics and Engineering
243 (2014) 2389 – 2400

INTERNATIONAL eJOURNAL OF MATHEMATICS AND ENGINEERING

www.InternationaleJournals.com

STAND-ALONE DISTRIBUTED GENERATION SYSTEM WITH AN ADAPTIVE CONTROLLER BASED VSC

Kunta Srinivas, D. Rajababu and C. Venkatesh

Department of EEE, SR Engineering College, Warangal, A.P.
cnuchinnu.kunta@gmail.com, durgamrajababu@gmail.com, challacvs@yahoo.com

Kunta Srinivas, M.Tech Student, Dept. of EEE, SR Engg.College,Warangal,AP.,cnuchinnu.kunta@gmail.com*
D.Rajababu, Associate Professor, Dept. of EEE, SR Engg.College, Warangal, AP., durgamrajababu@gmail.com
Dr. C. Venkatesh, Professor & HOD, Dept. of EEE, SR Engg.College, Warangal,AP.,challacvs@yahoo.com

***Abstract*— This paper proposes an adaptive control method of three-phase inverters for stand-alone distributed generation systems (DGSs) with and without controller. The proposed voltage controller includes two control terms: an adaptive compensating term and a stabilizing term. The adaptive compensating control term is constructed to avoid directly calculating the time derivatives of state variables. Meanwhile, the stabilizing control term is designed to asymptotically stabilize the error dynamics of the system. Also, a fourth-order optimal load current observer is proposed to reduce the number of current sensors and enhance the system reliability and cost effectiveness. The stability of the proposed voltage controller and the proposed load current observer is fully proven by using Lyapunov theory. The proposed control system can establish good voltage regulation such as fast dynamic response, small steady-state error, and low total harmonic distortion under sudden load change.**

***Keywords:*-Adaptive control, distributed generation (DG), distributed generation system (DGS), load current observer, stand-alone, three-phase inverter and voltage control.**

I. INTRODUCTION

DISTRIBUTED generation systems (DGSs) using renewable energy sources (such as wind turbines, photovoltaic arrays, biomass, and fuel cells) are gaining more and more attention in electric power industry to replace existing fossil fuels and reduce global warming gas emissions. Nowadays, the DGSs are extensively used in grid-connected applications, but they are more economical in a stand-alone operation in the case of rural villages or remote islands because connecting to the grid may lead to higher cost [1]–[5].

In stand-alone applications, the load-side inverter of the DGS operates analogous to an uninterruptible power supply (UPS) for its local loads [6]. Control of stand-alone DGSs or UPSs has been an attractive research area in recent years. In

these applications, the regulation performance of inverter output voltage is evaluated in terms of transient response time, steady-state error, and total harmonic distortion (THD). Furthermore, the quality of inverter output voltage is heavily affected by the types of loads such as sudden load change, unbalanced load, and nonlinear load. In [7], a conventional proportional–integral (PI) controller has been investigated. However, the output voltage has a considerable amount of the steady-state error, and its THD is not satisfactory in the case of nonlinear load. The $H\infty$ loop-shaping control scheme which is presented in [8] also cannot effectively mitigate the THD of the output voltage under nonlinear load. Therefore, the load-side inverters require advanced control techniques to achieve excellent voltage regulation performance, particularly under sudden load disturbance, unbalanced load, and nonlinear load.

Recently, various advanced control methods have been applied to the load-side inverters in DGS and UPS applications [6], [9]–[23]. In [9]–[11], a repetitive control is used to regulate UPS inverters, but the general problem with a repetitive control is its slow response and lack of systematical method to stabilize the error dynamics. Feedback linearization control techniques are proposed in [12] and [13]. Although these methods can achieve high performance of the output voltage, the control design techniques seem to be complicated. Two iterative learning control strategies are presented in [14], and these methods are capable of achieving high performance. However, the switching frequency of the inverter is very high, so it results in huge switching losses. In [15], a model predictive control with a load current observer is proposed. Although the control technique is simple, the THD of the output voltage is still high. In [16], another predictive control is proposed, but nonlinear load is not investigated. In [17], a robust PI controller is proposed for an autonomous DG unit. A full set of results is presented in the case of unbalanced RLC load, but the results about nonlinear load are not presented. Sliding-mode control techniques are applied for inverters in [18]–[21]. In [19]–[21], although good performance can be obtained, the controller designs are only for single-phase inverters [19], [20], and the results of nonlinear load are not presented [21]. In [6], a robust servomechanism control (RSC) is used to control three-phase inverters of a DGS in stand-alone mode. Even though this control technique can achieve good performance, it is quite complicated and needs exact parameter values of an RLC load. In [22] and [23], the authors propose the control strategies that consist of an RSC in an outer loop and a sliding-mode control in an inner loop. Even if the simulation results show good voltage performance, the control approach is complicated.

This paper proposes an adaptive voltage controller and an optimal load current observer of three-phase inverters for standalone DGSs. Also, it is analytically proven that the proposed voltage controller and the proposed load current observer are asymptotically stable, respectively. The proposed control method can achieve excellent voltage regulation such as fast transient behavior, small steady-state error, and low THD under sudden load change, unbalanced load, and nonlinear load.

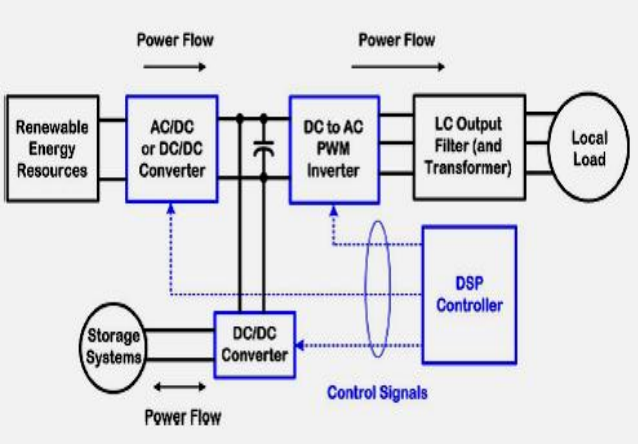

Fig.1. Configuration of a typical DGS in a stand-alone operation.

The remaining part of this paper is organized as follows. Section II describes the DGS in a stand-alone operation and the state-space model of the load-side inverter. The design and stability analysis of the proposed adaptive voltage controller are fully addressed in Section III. Section IV illustrates the proposed load current observer and analyzes its stability. In Section V, the simulation and experimental results are given to evaluate the

performance of the proposed control algorithm. Finally, conclusions are drawn in Section VI.

II. SYSTEM DESCRIPTION AND MATHEMATICAL MODEL

The configuration of a typical DGS in a stand-alone operation is shown in Fig. 1. It consists of renewable energy sources (e.g., wind turbines, solar cells, and fuel cells), an ac–dc power converter (wind turbines) or a unidirectional dc–dc boost converter (solar cells or fuel cells), a three-phase dc–ac inverter, an LC output filter, a DSP control unit, and a local load. As shown in Fig. 1, a transformer can be used to provide an electrical isolation or boost the output voltage of the three phase inverter, but it may lead to higher cost and larger volume. Also, storage systems such as batteries, ultra capacitors, and flywheels may be used to generate electric power during the transient (e.g., start-up or sudden load change) and improve the reliability of renewable energy sources.

In this paper, we deal with the voltage controller design of the three-phase inverter for stand-alone DGSs that can assure excellent voltage regulation (i.e., fast transient response, small steady-state error, and low THD) under sudden load change, unbalanced load, and nonlinear load. Thus, renewable energy sources and ac–dc power converters or unidirectional dc–dc boost converters can be replaced with a dc voltage source (V_{dc}).

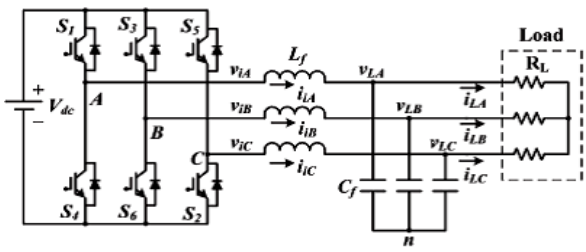

Fig.2. Circuit diagram of a three-phase inverter with an LC output filter for stand-alone DGSs.

Fig. 2 shows the circuit model of a three-phase inverter with an LC output filter for stand-alone DGSs. As shown in Fig. 2, the system comprises four parts: a dc voltage source (V_{dc}), a three-phase pulse-width modulation (PWM) inverter (S_1–S_6), an output filter (L_f and C_f), and a three-phase load (RL). Note that the LC filter is required to suppress high-order harmonic components of the inverter output voltage due to the PWM action and then provide the load with sinusoidal voltages.

The circuit model in Fig. 2 uses the following quantities. The inverter output lines to neutral voltage and phase current vectors are given by $\mathbf{V}_i = [v_{iA}\ v_{iB}\ v_{iC}]^T$ and $\mathbf{I}_i = [i_{iA}\ i_{iB}\ i_{iC}]^T$, respectively. In addition, the load lines to neutral voltage and phase current are represented by the vectors $\mathbf{V}_L = [v_{LA}\ v_{LB}\ v_{LC}]^T$ and $\mathbf{I}_L = [i_{LA}\ i_{LB}\ i_{LC}]^T$, respectively.

Assume that the three-phase voltages and currents used in Fig. 2 are balanced. By applying Kirchoff 's current law and Kirchoff 's voltage law at the LC output filter, the following voltage and current equations can be derived:

$$\begin{cases} \frac{d\mathbf{V}_L}{dt} = \frac{1}{C_f}\mathbf{I}_i - \frac{1}{C_f}\mathbf{I}_L \\ \frac{d\mathbf{I}_i}{dt} = \frac{1}{L_f}\mathbf{V}_i - \frac{1}{L_f}\mathbf{V}_L. \end{cases} \quad (1)$$

Under balanced conditions, the aforementioned state equations (1) in the stationary abc reference frame can be transformed to the equations in the stationary αβ reference frame by using the following expression [2], [3]:

$$\mathbf{X}_{\alpha\beta} = x_a e^{j0} + x_b e^{j\frac{2\pi}{3}} + x_c e^{j\frac{4\pi}{3}} \quad (2)$$

where $\mathbf{X}_{\alpha\beta} = x_\alpha + jx_\beta$.

Thus, the state equations (1) can be transformed to the following:

$$\begin{cases} \frac{d\mathbf{V}_{L\alpha\beta}}{dt} = \frac{1}{C_f}\mathbf{I}_{i\alpha\beta} - \frac{1}{C_f}\mathbf{I}_{L\alpha\beta} \\ \frac{d\mathbf{I}_{i\alpha\beta}}{dt} = \frac{1}{L_f}\mathbf{V}_{i\alpha\beta} - \frac{1}{L_f}\mathbf{V}_{L\alpha\beta} \end{cases} \quad (3)$$

where $\mathbf{V}_{L\alpha\beta} = [v_{L\alpha}\ v_{L\beta}]^T$, $\mathbf{I}_{L\alpha\beta} = [i_{L\alpha}\ i_{L\beta}]^T$, $V_{i\alpha\beta} = [v_{i\alpha}\ v_{i\beta}]^T$, and $I_{i\alpha\beta} = [i_{i\alpha}\ i_{i\beta}]^T$.

Next, the state equations in the stationary αβ reference frame can be transformed to the equations in the synchronously rotating dq reference frame from the following formula:

$$\mathbf{X}_{dq} = x_d + jx_q = \mathbf{X}_{\alpha\beta}e^{-j\theta} \quad (4)$$

where $\theta(t) = \int_0^t \omega(\tau)d\tau + \theta_0$ is the transformation angle, ω is the angular frequency ($\omega = 2\pi \cdot f$), and f is the fundamental frequency of voltage or current.

Finally, (3) can be transformed to

$$\begin{cases} \frac{d\mathbf{V}_{Ldq}}{dt} + j\omega\mathbf{V}_{Ldq} = \frac{1}{C_f}\mathbf{I}_{idq} - \frac{1}{C_f}\mathbf{I}_{Ldq} \\ \frac{d\mathbf{I}_{idq}}{dt} + j\omega\mathbf{I}_{idq} = \frac{1}{L_f}\mathbf{V}_{idq} - \frac{1}{L_f}\mathbf{V}_{Ldq} \end{cases} \quad (5)$$

where $\mathbf{V}_{Ldq} = [v_{Ld}\ v_{Lq}]^T$, $\mathbf{I}_{Ldq} = [i_{Ld}\ i_{Lq}]^T$, $\mathbf{V}_{idq} = [v_{id}\ v_{iq}]^T$, and $\mathbf{I}_{idq} = [i_{id}\ i_{iq}]^T$.

Also, (5) can be rewritten as follows:

$$\begin{cases} \dot{v}_{Ld} = \omega v_{Lq} - \frac{1}{C_f}i_{Ld} + \frac{1}{C_f}i_{id} \\ \dot{v}_{Lq} = -\omega v_{Ld} - \frac{1}{C_f}i_{Lq} + \frac{1}{C_f}i_{iq} \\ \dot{i}_{id} = -\frac{1}{L_f}v_{Ld} + \omega i_{iq} + \frac{1}{L_f}v_{id} \\ \dot{i}_{iq} = -\frac{1}{L_f}v_{Lq} - \omega i_{id} + \frac{1}{L_f}v_{iq} \end{cases} \quad (6)$$

where $\dot{v}_{Ld}$, $\dot{v}_{Lq}$, $\dot{i}_{id}$, and $\dot{i}_{iq}$ denote the time derivatives of v_{Ld}, v_{Lq}, i_{id}, and i_{iq}, respectively.

Note that V_{Ldq} and I_{idq} are the state variables, V_{idq} is the control input, and I_{Ldq} is defined as the disturbance.

In this paper, the following assumptions are made to design an adaptive controller and a load current observer.

1. v_{Ld}, v_{Lq}, i_{id}, and i_{iq} are available.
2. The desired load dq-axis voltages vL_{dref} and vL_{qref} are constant, and its derivatives can be set to zero.
3. i_{Ld} and i_{Lq} are unknown, and they change very slowly during the sampling period [15].

III. ADAPTIVE VOLTAGE CONTROLLER DESIGN AND STABILITY ANALYSIS

Based on the system model (6), this section fully addresses the proposed adaptive control algorithm and its stability analysis.

First, the errors of the load dq-axis voltages (v_{Ld} and v_{Lq}) and the inverter dq currents (i_{id} and i_{iq}) can be defined as

$$\bar{v}_{Ld} = v_{Ld} - v_{Ldref} \qquad \bar{v}_{Lq} = v_{Lq} - v_{Lqref}$$
$$\bar{i}_{id} = i_{id} - i_{idref} \qquad \bar{i}_{iq} = i_{iq} - i_{iqref} \quad (7)$$

where vL_{dref} and vL_{qref} are the reference values of v_{Ld} and v_{Lq}, respectively, and i_{idref} and i_{iqref} are the reference values of i_{id} and i_{iq}, respectively. Again, the i_{idref} and i_{iqref} are given by

$$i_{idref} = i_{Ld} - \omega C_f v_{Lq} \qquad i_{iqref} = i_{Lq} + \omega C_f v_{Ld}. \quad (8)$$

Next, the uncertainty terms u_d and u_q, which cannot be accurately computed in real system, can be defined as

$$\begin{cases} u_d = -\frac{\omega L_f}{\alpha_d}v_{Lq} + \frac{L_f}{C_f\alpha_d}i_{Ld} - \frac{L_f}{C_f\alpha_d}i_{id} - L_f\omega i_{iq} + L_f\dot{i}_{idref} \\ u_q = \frac{\omega L_f}{\alpha_q}v_{Ld} + \frac{L_f}{C_f\alpha_q}i_{Lq} + L_f\omega i_{id} - \frac{L_f}{C_f\alpha_q}i_{iq} + L_f\dot{i}_{iqref} \end{cases} \quad (9)$$

where α_d and α_q are positive numbers.

As shown in (9), it should be noted that u_d and u_q include the time derivatives $\dot{i}_{idref}$ and $\dot{i}_{iqref}$ which cannot be calculated directly because they are very noisy. In addition, assume that L_f has some uncertainties due to nonlinear magnetic properties. Therefore, the uncertainty terms u_d and u_q need to be correctly estimated in real time instead of straightforwardly computing the time derivatives of i_{idref} and i_{iqref} .

Then, the following error dynamics can be obtained:

$$\begin{cases} \dot{\bar{v}}_{Ld} = \frac{1}{C_f}\dot{\bar{i}}_{id} \\ \dot{\bar{v}}_{Lq} = \frac{1}{C_f}\dot{\bar{i}}_{iq} \\ \dot{\bar{v}}_{Ld} + \alpha_d\dot{\bar{i}}_{id} = -\frac{\alpha_d}{L_f}(u_d - v_{id} + v_{Ld}) \\ \dot{\bar{v}}_{Lq} + \alpha_q\dot{\bar{i}}_{iq} = -\frac{\alpha_q}{L_f}(u_q - v_{iq} + v_{Lq}). \end{cases} \quad (10)$$

The control inputs v_{id} and v_{iq} can be divided into the following two control terms:

$$\begin{cases} v_{id} = u_{ffd} + u_{fbd} \\ v_{iq} = u_{ffq} + u_{fbq} \end{cases} \quad (11)$$

where u_{ffd} (= u_d + v_{Ld}) and u_{ffq} (= u_q + v_{Lq}) are the d and q-axis compensation control terms and u_{fbd} and u_{fbq} are the d- and q-axis feedback control terms to stabilize the error dynamics of the system.

In order to establish this estimation law, let the following lemma be considered.

Lemma 1: Assume that (L_f $\dot{i}_{idref}$ + L_f $i_{Ld}/C_f\alpha_d$) and (L_f $\dot{i}_{iqref}$ + L_f $i_{Lq}/C_f\alpha_q$) slowly vary, so they can be set to the constant. There exist constant parameter

vectors $m^*_d = [m^*_{d1}, m^*_{d2}, m^*_{d3}, m^*_{d4}]^T$ and $m^*_q = [m^*_{q1}, m^*_{q2}, m^*_{q3}, m^*_{q4}]^T$ such that

$$p_d^T m_d^* = \sum_{i=1}^{4} p_{di} m_{di}^* = u_d \qquad p_q^T m_q^* = \sum_{i=1}^{4} p_{qi} m_{qi}^* = u_q \tag{12}$$

where $pd = [pd1, pd2, pd3, pd4]^T = [v_{Lq}, i_{id}, i_{iq}, 1]^T$ and $pq = [pq1, pq2, pq3, pq4]T = [v_{Ld}, i_{id}, i_{iq}, 1]^T$.

Proof: It is clear that (12) holds with

$$m_d^* = \left[-\frac{\omega L_f}{\alpha_d}, -\frac{L_f}{C_f \alpha_d}, -\omega L_f, L_f \dot{i}_{idref} + \frac{L_f}{C_f \alpha_d} i_{Ld}\right]^T$$

$$m_q^* = \left[\frac{\omega L_f}{\alpha_q}, \omega L_f, -\frac{L_f}{C_f \alpha_q}, L_f \dot{i}_{iqref} + \frac{L_f}{C_f \alpha_q} i_{Lq}\right]^T. \tag{13}$$

Therefore, the following theorem can be established.

Theorem1: Assume that C_f is known. Let the compensation control terms (u_{ffd} and u_{ffq}) and the feedback control terms (u_{fbd} and u_{fbq}) be calculated by the following adaptive control laws:

$$\begin{cases} u_{ffd} = \sum_{i=1}^{4} m_{di} p_{di} + v_{Ld}, & u_{fbd} = -\delta_d \sigma_d \\ u_{ffq} = \sum_{i=1}^{4} m_{qi} p_{qi} + v_{Lq}, & u_{fbq} = -\delta_q \sigma_q \end{cases} \tag{14}$$

where

$$m_{di} = -\frac{1}{\phi_{di}} \int_0^t p_{di} \sigma_d d\tau \qquad m_{qi} = -\frac{1}{\phi_{qi}} \int_0^t p_{qi} \sigma_q d\tau \tag{15}$$

$$\sigma_d = (\bar{v}_{Ld} + \alpha_d \bar{i}_{id}) \qquad \sigma_q = (\bar{v}_{Lq} + \alpha_d \bar{i}_{iq}) \tag{16}$$

αd and αq are positive design constants, m_{di} and m_{qi} are estimates of m^*_{di} and m^*_{qi}, $\delta_d > 0$, $\delta_q > 0$, $\varphi_{di} > 0$, and $\varphi_{qi} > 0$. Then, $\bar{v}_{Ld}$ and $\bar{v}_{Lq}$ converge to zero, and m_{di} and m_{qi} are bounded.

Proof: Let the Lyapunov function be defined as

$$V(t) = \sigma_d^2 + \sigma_q^2 + \sum_{i=1}^{4} \frac{\alpha_d}{L_f} \phi_{di} \bar{m}_{di}^2 + \sum_{i=1}^{4} \frac{\alpha_q}{L_f} \phi_{qi} \bar{m}_{qi}^2 \tag{17}$$

where $m_{di} = m^*_{di} - m_{di}$ and $m_{qi} = \xi^*_{qi} - \xi_{qi}$. Its time derivative is expressed as the following:

$$\dot{V} = 2\left(\sigma_d \dot{\sigma}_d + \sigma_q \dot{\sigma}_q - \sum_{i=1}^{4} \frac{\alpha_d}{L_f} \phi_{di} \bar{m}_{di} \dot{m}_{di} - \sum_{i=1}^{4} \frac{\alpha_q}{L_f} \phi_{qi} \bar{m}_{qi} \dot{m}_{qi}\right). \tag{18}$$

Also, the following equation can be obtained from (10) and (16):

$$\begin{cases} \dot{\sigma}_d = \frac{\alpha_d}{L_f}(v_{id} - u_d - v_{Ld}) \\ \dot{\sigma}_q = \frac{\alpha_q}{L_f}(v_{iq} - u_q - v_{Lq}). \end{cases} \tag{19}$$

On the other hand, *Lemma 1*, (11), (14), and (15) imply that

$$\begin{cases} v_{id} = -\delta_d \sigma_d + v_{Ld} - \sum_{i=1}^{4} \bar{m}_{di} p_{di} + u_d \\ v_{iq} = -\delta_q \sigma_q + v_{Lq} - \sum_{i=1}^{4} \bar{m}_{qi} p_{qi} + u_q \end{cases}$$

$$\begin{cases} \dot{m}_{di} = -\frac{1}{\phi_{di}} p_{di} \sigma_d \\ \dot{m}_{qi} = -\frac{1}{\phi_{qi}} p_{qi} \sigma_q \end{cases} \tag{20}$$

where the following equalities are used:

$$\sum_{i=1}^{4} m_{di} p_{di} = u_d - \sum_{i=1}^{4} \bar{m}_{di} p_{di}$$

$$\sum_{i=1}^{4} m_{qi} p_{qi} = u_q - \sum_{i=1}^{4} \bar{m}_{qi} p_{qi}.$$

Substituting (19) and (20) into (17) yields

$$\dot{V} = -2\left(\delta_d \frac{\alpha_d}{L_f} \sigma_d^2 + \delta_q \frac{\alpha_q}{L_f} \sigma_q^2\right) \le 0. \tag{21}$$

Integrating both sides of (20) gives

$$\int_0^\infty \dot{V}(\tau) d\tau \le -2\left(\delta_d \frac{\alpha_d}{L_f} \int_0^\infty \sigma_d^2 d\tau + \delta_q \frac{\alpha_q}{L_f} \int_0^\infty \sigma_q^2 d\tau\right)$$

or equivalently

$$V(\infty) - V(0) \le -2\left(\delta_d \frac{\alpha_d}{L_f} \int_0^\infty \sigma_d^2 d\tau + \delta_q \frac{\alpha_q}{L_f} \int_0^\infty \sigma_q^2 d\tau\right). \tag{22}$$

Thus, the aforementioned equation can be rewritten as

$$2\left(\delta_d\frac{\alpha_d}{L_f}\int_0^\infty \sigma_d^2 d\tau+\delta_q\frac{\alpha_q}{L_f}\int_0^\infty \sigma_q^2 d\tau\right)\le V(0)-V(\infty)\le V(0) \tag{23}$$

where V (t) ≥ 0 is used. Then, the following inequalities can be derived:

$$\int_0^\infty \sigma_d^2 d\tau<\infty \qquad \int_0^\infty \sigma_q^2 d\tau<\infty \tag{24}$$

which implies that $\sigma_d, \sigma_q \in L_2$. Since $\dot{V} \le 0$ as shown in (21), V (t) is non increasing and is upper bounded as V (t) ≤ V (0). This implies that $\sigma_d \in L_\infty$, $\sigma_q \in L_\infty$, $m_{qi} \in L_\infty$, and $m_{qi} \in L_\infty$.

Meanwhile, from the first two equations in (10), the σ_d and σ_q given in (16) can be rearranged as

$$\begin{cases}\sigma_d=(\bar{v}_{Ld}+C_f\alpha_d\dot{\bar{v}}_{Ld})\\ \sigma_q=(\bar{v}_{Lq}+C_f\alpha_q\dot{\bar{v}}_{Lq}).\end{cases} \tag{25}$$

Then, the transfer functions $H_d(s)$ from σ_d to $\bar{v}_{Ld}$ and $H_q(s)$ from σ_q to $\bar{v}_{Lq}$ are given by the following strictly positive functions:

$$H_d(s)=\frac{1}{(1+C_f\alpha_d s)} \qquad H_q(s)=\frac{1}{(1+C_f\alpha_q s)}. \tag{26}$$

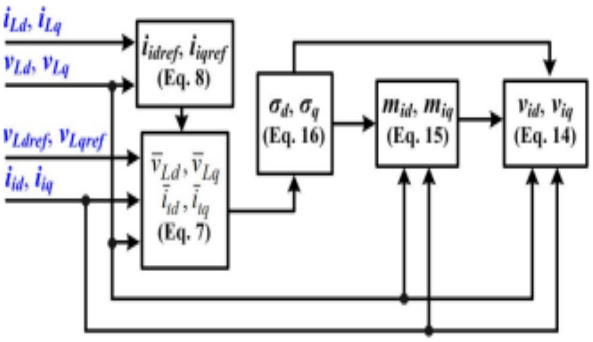

Fig.3 Block diagram of the proposed adaptive voltage control scheme

Therefore, by [24], it can be concluded that $\bar{v}_{Ld}$ and $\bar{v}_{Lq}$ converge to zero.

Remark 1: This remark discusses how the controller gains are chosen. The adaptive gains m_{di} and m_{qi} are incorporated in the compensation control terms u_{ffd} and u_{ffq} as depicted in (14). To realize the fast convergence and transient response, the adaptive gains are tuned to large values. Since these adaptive gains are inversely related to φdi and φqi as in (15), the smaller the values selected for φ_{di} and φ_{qi}, the more likely that it will result in larger values of the adaptive gains. On the other hand, with the feedback terms ufbd and ufbq given in (14), σ_d and σ_q are further defined in (25), and these feedback terms can be regarded as a proportional–differential (PD) controller. In this context, the control parameters α_d, α_q, δ_d, and δ_q can be decided based on the tuning rule in [25]. Finally, the parameters α_d, α_q, δ_d, δ_q, φ_{di}, and φ_{qi} can be tuned by the following procedure: 1) By utilizing the tuning rule in [25], tune the parameters α_d, α_q, δ_d, and δ_q; 2) set quite large values for φ_{di} and φ_{qi}; 3) reduce φ_{di} and φ_{qi} by a small amount; and 4) if the acceptable transient performance is attained by current control parameters, then quit, or otherwise, return to step 3.

Remark 2: As shown in (14), the proposed voltage controller includes two parts: feedback terms and adaptive compensation terms. The function of the feedback terms is to stabilize the error dynamics of the system. On a separate note, the adaptive compensation terms take into acount not only parameter uncertainties but also noises. Therefore, the proposed control technique can attain good performance with the existence of parameter uncertainties and noises in practice.

Fig.3 shows the block diagram of the proposed adaptive voltage control scheme.

IV. LOAD CURRENT OBSERVER DESIGN AND STABILITY ANALYSIS

In Fig. 3, it is clear that the proposed adaptive controller needs load current information. Using the current sensors to measure the load currents ($\mathbf{I}_L$) makes the system more expensive and less reliable. In this section, a linear optimal load current observer is designed to accurately estimate load current information that can heavily affect the controller performance. Based on Assumption 3 and

the first two equations in (6), a fourth-order dynamic model can be obtained as follows:

$$\dot{x} = Ax + Bu \tag{27}$$

where

$$x = \begin{bmatrix} i_{Ld} \\ i_{Lq} \\ v_{Ld} \\ v_{Lq} \end{bmatrix} \qquad A = \begin{bmatrix} 0 & 0 & 0 & 0 \\ 0 & 0 & 0 & 0 \\ -1/C_f & 0 & 0 & \omega \\ 0 & -1/C_f & -\omega & 0 \end{bmatrix}$$

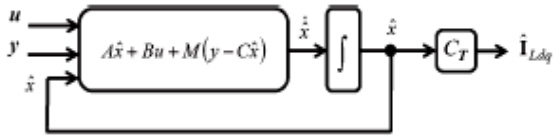

Fig.4. Block diagram of the proposed optimal load current observer.

$$B = \begin{bmatrix} 0 & 0 \\ 0 & 0 \\ 1/C_f & 0 \\ 0 & 1/C_f \end{bmatrix} \qquad u = \begin{bmatrix} i_{id} \\ i_{iq} \end{bmatrix}.$$

Then, the load current observer model can be represented as

$$\dot{\hat{x}} = A\hat{x} + My - MC\hat{x} + Bu$$

$$y = Cx$$

$$\hat{\mathbf{I}}_{Ldq} = \begin{bmatrix} \hat{i}_{Ld} \\ \hat{i}_{Lq} \end{bmatrix} = C_T\hat{x} \tag{28}$$

where $\hat{i}_{Ld}$ and $\hat{i}_{Lq}$ are estimates of i_{Ld} and i_{Lq}, respectively, $M \in R^{4\times2}$ is an observer gain matrix, and

$$\hat{x} = \begin{bmatrix} \hat{i}_{Ld} \\ \hat{i}_{Lq} \\ \hat{v}_{Ld} \\ \hat{v}_{Lq} \end{bmatrix} \quad C = \begin{bmatrix} 0 & 0 & 1 & 0 \\ 0 & 0 & 0 & 1 \end{bmatrix} \quad C_T = \begin{bmatrix} 1 & 0 & 0 & 0 \\ 0 & 1 & 0 & 0 \end{bmatrix}.$$

Fig. 4 shows the block diagram of the proposed load current observer.

Next, the error dynamics of the load current observer can be obtained as follows:

$$\dot{\tilde{x}} = (A - MC)\tilde{x} \tag{29}$$

where $x = x - \hat{x}$.

Theorem 2: Consider the following algebraic Riccati equation:

$$AP + PA^{T} - PC^{T}R^{-1}CP + Q = 0 \tag{30}$$

where $Q \in R^{4\times4}$ is a symmetric positive semi definite matrix, $R \in R^{2\times2}$ is a symmetric positive definite matrix, and
$P \in R^{4\times4}$ is a solution matrix. Also, assume that the load current observer gain matrix M is given by

$$M = PC^{T}R^{-1}. \tag{31}$$

Then, the estimation error converges exponentially to zero.

Proof: Let us define the Lyapunov function as $Vo(\_x) = \_xTX\_x$, where $X = P^{-1}$. Its time derivative along the error dynamics (29) is given by

$$\begin{aligned} \dot{V}_o(\tilde{x}) &= \frac{d}{dt}\tilde{x}^{T}X\tilde{x} = 2\tilde{x}^{T}(XA - XPC^{T}R^{-1}C)\tilde{x} \\ &= \tilde{x}^{T}X(AP + PA^{T} - 2PC^{T}R^{-1}CP)X\tilde{x} \\ &\le -\tilde{x}^{T}XQX\tilde{x}. \end{aligned} \tag{32}$$

This implies that $x\tilde{}$ *is* exponentially stable.

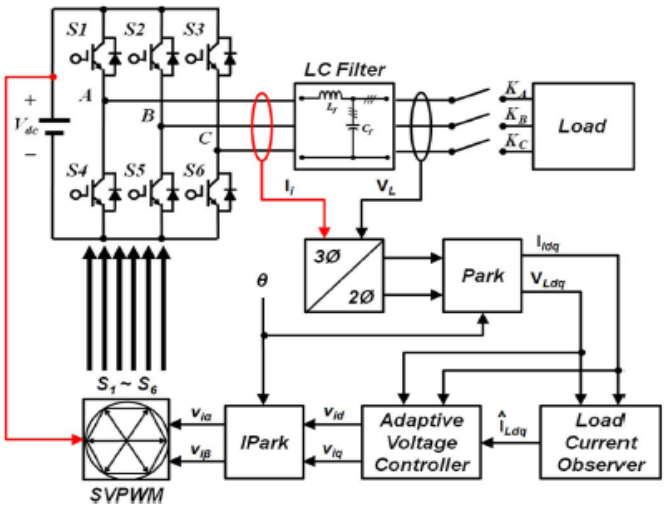

Fig.5. Overall block diagram of the proposed adaptive control system.

Remark 3: The proposed fourth-order load current observer is the Kalman–Bucy optimal observer which minimizes the performance index $E(\_x^{T}\_x)$

representing the expectation value of $\_x^T\_x$ for the following perturbed model:

$$\dot{x} = Ax + Bu + d \qquad y = Cx + v \tag{33}$$

where $d \in R^4$ and $v \in R^2$ are independent white Gaussian noise signals with E(d) = 0, E(v) = 0, $E(dd^T) = Q$, and $E(vv^T) = R$.

Remark 4: By referring to [26], this remark details on how the observer gain matrix M is determined. Normally, the observer performance is mostly influenced by the system model if the measurements are excessively noisy (large R) and the input noise intensity is small (small Q). On that note, M is small. This leads to a slow observer as measured by the location of its eigen values. However, if the measurements are good and the input noise intensity is large, the observer relies on the measurement. In this case, M is large, resulting in a fast observer with high bandwidth. Consequently, by assuming that the measurement is good, the fast observer is desirable. Lastly, the subsequent procedure summarizes the tuning process of the observer gain matrix M: 1) Set Q and R as identity matrices; 2) gradually increase Q and decrease R, and then, calculate M as in (30) and (31); and 3) unless the observer performance is satisfied, return to step 2, or otherwise, quit.

V.PERFORMANCE EVALUATION WITH AND WITHOUT THE PROPOSED CONTROLLER

In this section, simulations are made, and various results with and without the proposed controller are presented. To evaluate the performance of the proposed observer-based adaptive control system, a power level 200-kVA class is studied because the 200-kVA unit is a too high power level to build in the laboratory. In this paper, simulations are performed by using Mat lab/Simulink software.

Fig.5 shows the schematic diagram of the proposed adaptive voltage control approach. As shown in Fig. 5, the inverter currents ($\mathbf{I}_i$) and load output voltages ($\mathbf{V}_L$) are measured with sensors and then transformed to the quantities $\mathbf{I}_{idq}$ and $\mathbf{V}_{Ldq}$ in the synchronously rotating dq reference frame, respectively. On the other hand, the load currents ($\mathbf{I}_{Ldq}$) can be estimated by using the proposed current observer. In this paper, a space-vector PWM technique is utilized to approximate the reference voltages and supply less harmonic voltages to the load. Simulations and experiments are accomplished to demonstrate the transient performance of the proposed control algorithm under the following two different cases:

Case 1) balanced resistive load (transient behavior—0% to 100%);
Case 2) balanced resistive load (transient behavior—100% to 0%);

TABLE I
SYSTEM PARAMETERS OF A 200-kVA UNIT

DGS rated power	200 kVA
dc-link voltage (V_{dc})	600 V
Switching & sampling frequency	4 kHz
Load output voltages ($\mathbf{V}_{L,\,rms}$)	220 V
Fundamental frequency (f)	60 Hz
Output filter capacitance (C_f)	500 μF
Output filter inductance (L_f)	0.3 mH

A. 200-kVA Unit

Consider a 200-kVA DG unit, and the system parameters are given in Table I.

As shown in Table I, a three-phase LC output filter is designed with L_f =0.3mH and C_f =500μF, and it has a cutoff frequency of 410.9 Hz. It is well known that, the larger the values of L_f and C_f, the better the filter performance. However, large L_f leads to higher cost and larger volume. Also, large C_f results in larger capacitor current at no load in addition to higher cost. Therefore, there exists a tradeoff when selecting L_f and C_f.

In this case, the controller gains and observer gain matrix are selected as follows: $\alpha_d=\alpha_q= 0.1$, $\varphi_{di}=\varphi_{qi}$ =1000,

$\delta_d = \delta_q = 1000$, and

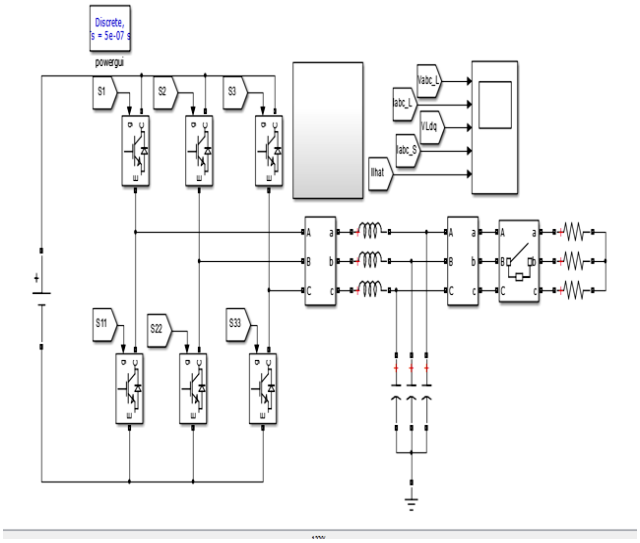

Fig.6 simulink model

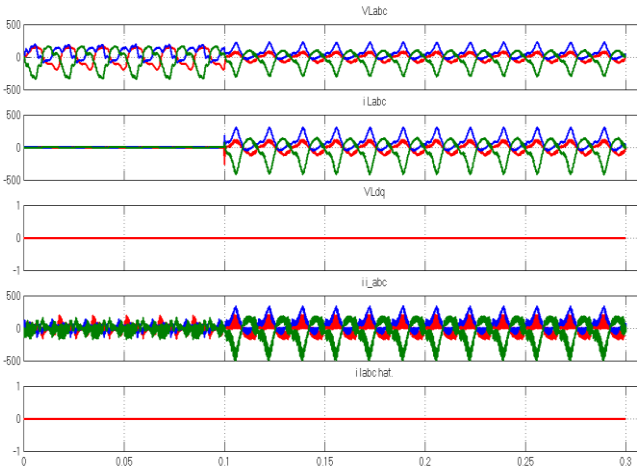

Fig.7. Simulation results without the proposed control scheme under Case 1 for a 200-kVA unit (balanced resistive load: 0%–100%).

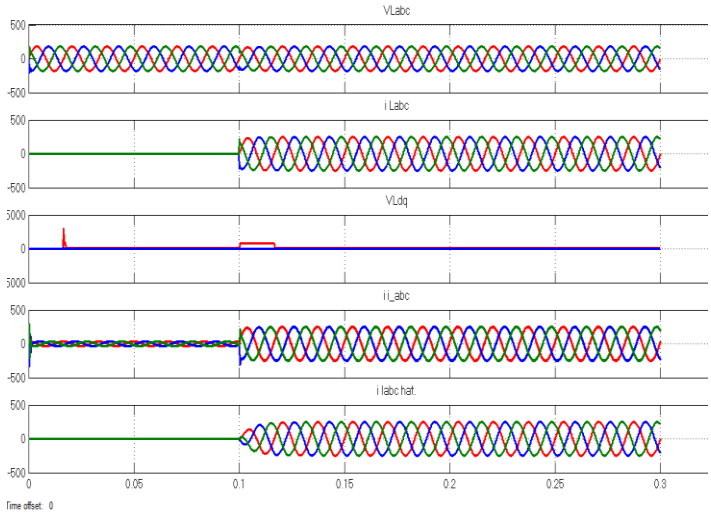

Fig.8. Simulation results of the proposed control scheme under Case 1 for a 200-kVA unit (balanced resistive load: 0%–100%).

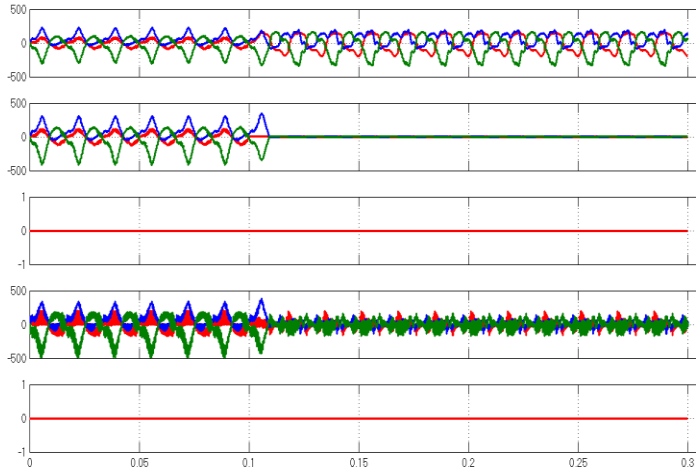

Fig.9. Simulation results without the proposed control scheme under Case 2 for a 200-kVA unit (balanced resistive load: 100% to 0%).

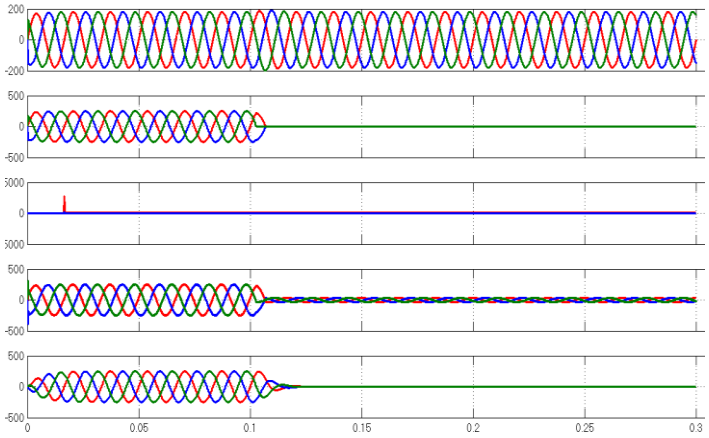

Fig.10. Simulation results of the proposed control scheme under Case 2 for a 200-kVA unit (balanced resistive load: 100% to 0%).

$$M = 10^4 \times \begin{bmatrix} -0.3162 & -0.0039 & 3.0955 & -0.0000 \\ 0.0039 & -0.3162 & -0.0000 & 3.0955 \end{bmatrix}^{\mathrm{T}}.$$

Note that these parameters are chosen through extensive simulation studies with the aforementioned procedures in Remark 1 and Remark 4.

Figs. 6–10 show the simulation results without the proposed control technique & with the proposed control technique under Cases 1, 2 for a 200-kVA unit, respectively. Each figure shows the waveforms of load voltages ($\mathbf{V}_L$), inverter currents ($\mathbf{I}_i$), load currents ($\mathbf{I}_L$), estimated load currents ($\hat{\mathbf{I}}_L$), control inputs (v_{id} and v_{iq}), and load current error ($e_{LA} = i_{LA} - \hat{i}_{LA}$). In Fig.6, a 0.726-Ω resistor is used for a balanced resistive load. Figs.7-10 show the transient performance under a balanced resistive load, and the load voltage waveforms are only slightly distorted during the transients and return to steady state within 0.52ms. In both figures, the voltage waveforms look quite sinusoidal throughout the time. In Figs. 7–10, it is seen that the proposed observer accurately estimates the load currents under two load scenarios.

From all simulation results, it can be concluded that the proposed control technique can attain exceptional voltage regulation performance such as more stable output voltage and lower THD under various load types.

VI. CONCLUSION

In this paper, an adaptive voltage controller has been proposed for a three-phase PWM inverter of stand-alone DGSs. Load current information was estimated by a fourth-order optimal observer. The stability of the proposed controller and observer was analytically proven by applying Lyapunov stability theory. This adaptive control strategy can achieve more stable output voltage and lower THD under sudden load change. The simulation results without the proposed controller are also given and compared. The effectiveness and feasibility of the proposed control strategy were verified through various simulation results.

REFERENCES

[1]Ton Duc Do, Viet Quoc Leu, Young-Sik Choi, Han Ho Choi, and Jin-Woo Jung, " An Adaptive Voltage Control Strategy Of Three-Phase Inverter For Stand-Alone Distributed Generation Systems," IEEE Trans. Ind. Electron., vol. 60, no. 12, pp. 5660–5672, Dec. 2013.

[2]F. Blaabjerg, R. Teodorescu, M. Liserre, and A. V. Timbus, "Overview of control and grid synchronization for distributed power generation systems," IEEE Trans. Ind. Electron., vol. 53, no. 5, pp. 1398–1409, Oct. 2006.

[2] A. Yazdani, "Control of an islanded distributed energy resource unit with load compensating feed-forward," in Proc. IEEE PES Gen. Meeting, Aug. 2008, pp. 1–7.

[3] K. L. Nguyen, D. J. Won, S. J. Ahn, and I. Y. Chung, "Power sharing method for a grid connected microgrid with multiple distributed generators," J. Elect. Eng. Technol., vol. 7, no. 4, pp. 459–467, Jul. 2012.

[4] H. C. Seo and C. H. Kim, "Analysis of stability of PV system using the eigenvalue according to the frequency variation and requirements of frequency protection," J. Elect. Eng. Technol., vol. 7, no. 4, pp. 480–485, Jul. 2012.

[5] I. S. Bae and J. O. Kim, "Phasor discrete particle swarm optimization algorithm to configure micro-grids," J. Elect. Eng. Technol., vol. 7, no. 1, pp. 9–16, Jan. 2012.

[6] H. Karimi, E. J. Davision, and R. Iravani, "Multivariable servomechanism controller for autonomous operation of a distributed generation unit: Design and performance evaluation," IEEE Trans. Power Syst., vol. 25, no. 2, pp. 853–865, May 2010.

[7] U. Borup, P. N. Enjeti, and F. Blaabjerg, "A new space-vector-based control method for UPS systems powering nonlinear and unbalanced loads," IEEE Trans. Ind. Appl., vol. 37, no. 6, pp. 1864–1870, Nov./Dec. 2001.

[8] T. S. Lee, S. J. Chiang, and J. M. Chang, " H∞ loop-shaping controller designs for the single-phase UPS inverters," IEEE Trans. Power Electron., vol. 16, no. 4, pp. 473–481, Jul. 2001.

[9] G. Escobar, A. M. Stankovic, and P. Mattavelli, "An adaptive controller in stationary reference frame for d-statcom in unbalanced operation," IEEE Trans. Ind. Electron., vol. 51, no. 2, pp. 401–409, Apr. 2004.

[10] P. Mattavelli, G. Escobar, and A.M. Stankovic, "Dissipativity-based adaptive and robust control of UPS," IEEE Trans. Ind. Electron., vol. 48, no. 2, pp. 334–343, Apr. 2001.

[11] R. Escobar, A. A. Valdez, J. Leyva-Ramos, and P. Mattavelli, "Repetitivebased controller for a UPS inverter to compensate unbalance and harmonic distortion," IEEE Trans. Ind. Electron., vol. 54, no. 1, pp. 504–510, Feb. 2007.

[12] D. E. Kim and D. C. Lee, "Feedback linearization control of three-phase UPS inverter systems," IEEE Trans. Ind. Electron., vol. 57, no. 3, pp. 963– 968, Mar. 2010.

[13] A. Houari, H. Renaudineau, J. P. Pierfedrici, and F.Meibody-Tabar, "Flatness based control of three phase inverter with output LC filter," IEEE Trans. Ind. Electron., vol. 59, no. 7, pp. 2890–2897, Jul. 2012.

[14] H. Deng, R. Oruganti, and D. Srinivasan, "Analysis and design of iterative learning control strategies for UPS inverters," IEEE Trans. Ind. Electron., vol. 54, no. 3, pp. 1739–1751, Jun. 2007.

[15] P. Cortés, G. Ortiz, J. I. Yuz, J. Rodrisguez, S. Vazquez, and L. G. Franquelo, "Model predictive control of an inverter with output LC filter for UPS applications," IEEE Trans. Ind. Electron., vol. 56, no. 6, pp. 1875–1883, Jun. 2009.

[16] K. H. Ahmed, A. M. Massoud, S. J. Finney, and B. W. Williams, "A modified stationary reference frame-based predictive current control with zero steady-state error for LCL coupled inverter-based distributed generation systems," IEEE Trans. Ind. Electron., vol. 58, no. 4, pp. 1359–1370, Apr. 2011.

[17] H. Karimi, A. Yazdani, and R. Iravani, "Robust control of an autonomous four-wire electronically-coupled distributed generation unit," IEEE Trans. Power Del., vol. 26, no. 1, pp. 455–466, Jan. 2011.

[18] T. L. Tai and J. S. Chen, "UPS inverter design using discrete-time sliding-mode control scheme," IEEE Trans. Ind. Electron., vol. 49, no. 1, pp. 67–75, Feb. 2002.

[19] O. Kukrer, H. Komurcugil, and A. Doganalp, "A three-level hysteresis function approach to the sliding-mode control of single-phase UPS inverters," IEEE Trans. Ind. Electron., vol. 56, no. 9, pp. 3477–3486, Sep. 2009.

[20] H. Komurcugil, "Rotating sliding line based sliding mode control for single-phase UPS inverters," IEEE Trans. Ind. Electron., vol. 59, no. 10, pp. 3719–3726, Oct. 2012.

[21] R. J. Wai and C. Y. Lin, "Dual active low-frequency ripple control for clean-energy power-conditioning mechanism," IEEE Trans. Ind.

Electron., vol. 58, no. 11, pp. 5172–5185, Nov. 2011.

[22] M. Dai, M. N. Marwali, J. W. Jung, and A. Keyhani, "A three-phase fourwire inverter control technique for a single distributed generation unit in island mode," IEEE Trans. Power Electron., vol. 23, no. 1, pp. 322–331, Jan. 2008.

[23] M. N. Marwali and A. Keyhani, "Control of distributed generation systems—Part I: Voltages and currents control," IEEE Trans. Power Electron., vol. 19, no. 6, pp. 1541–1550, Nov. 2004.

[24] F. L. Lewis, C. T. Abdallah, and D. M. Dawson, Control of Robot Manipulators. New York: MacMillan, 1993.

[25] K. J. Astrom and B.Witternmark, Computer-Controlled Systems—Theory and Design. Englewood Cliffs, NJ: Prentice-Hall, 1990.

[26] B. Shahian and M. Hassul, Control System Design Using Matlab. Englewood Cliffs, NJ: Prentice-Hall, 1993.